

Influence of Cross-sectional Configuration on the Synchronization of Kármán Vortex Shedding with the Cylinder Oscillation*

Mizuyasu KOIDE**, Shouji TOMIDA***

Tsutomu TAKAHASHI**, László BARANYI****

and Masataka SHIRAKASHI**

The influence of cross-sectional configuration of a cylindrical body on the lock-in phenomenon of Kármán vortex shedding was investigated using a mechanical oscillator for cross-flow oscillation of the cylinder. A circular, a semi-circular and a triangular cylinder with an equal height were used as test cylinders to see the effect of the movement of the separation point. The lock-in criteria accounting for the spanwise coherency of the Kármán vortex were discussed based on the experimental data under a fixed Reynolds number of around 3 500. The lock-in region on the plane of non-dimensional cylinder frequency and the non-dimensional amplitude was almost the same for all of the cylinders in spite of differences in the range of the separation point movement. The minimum value of non-dimensional threshold amplitude for lock-in was much smaller than the value of 0.05 which was reported so far. Results obtained in this work imply that the movement of the separation point is a result of the lock-in phenomenon, rather than an essential cause.

Key Words : Flow Induced Vibration, Kármán Vortex, Flow Visualization, Flow Separation, Cross-Sectional Configuration, Synchronization, Lock-In

1. Introduction

It is well known that the Kármán vortex sheds periodically from cylindrical bodies with a blunt cross section shape under a wide range of flow conditions. Since Kármán vortex shedding generates alternating lift force exerting on the cylinder, it can induce large cross flow oscillation when the natural frequency of the elastically supported cylinder is around the vortex shedding frequency from the fixed cylinder. Such

vibrations caused by the hydrodynamic force which originates from periodic vortex formation and shedding are called vortex excitation. Since the Kármán vortex excitation is observed frequently at bridges, maritime structures, fluid machinery and so on, and sometimes causes structural damage, enormous efforts have been devoted to clarifying its mechanism and to controlling it.

In addition to its practical importance, the Kármán vortex excitation is an interesting phenomenon from the viewpoint of fluid dynamics, because it is a non-linear self-excitation oscillation caused by the interaction between the body motion and the flow around it. Hence, numerous research papers have been reported on this subject as seen in reviews of Sarpkaya⁽¹⁾ and Griffin and Hall⁽²⁾. Of particular interest is the phenomenon of synchronization, in which the frequency of vortex shedding coincides with that of the cylinder oscillation. This is also known as lock-in.

* Received 22nd August, 2001

** Department of Mechanical Engineering, Nagaoka University of Technology, 1603-1 Kamitomiokamachi, Nagaoka, Niigata 940-2188, Japan. E-mail: mkoide@mech.nagaokaut.ac.jp

*** Instruments, HITACHI, Ltd., 882 Ichige, Hitachinaka, Ibaraki 312-8504, Japan

**** Department of Fluid and Heat Engineering, University of Miskolc, H-3515, Miskolc-Egyetemvaros, Hungary

Funakawa⁽³⁾ showed that the separation point on oscillating circular cylinder moves forward and backward, synchronizing with the oscillation. Based on this observation he suggested a self-excitation mechanism for the Kármán vortex excitation. Koopman⁽⁴⁾ investigated the lock-in region in terms of the oscillation amplitude A and the frequency of a circular cylinder f_c . He showed that the Kármán vortex is more likely to lock-in when f_c is closer to the vortex shedding frequency from the fixed cylinder, f_{v0} , i.e. the threshold amplitude is lower when f_c/f_{v0} is closer to unity. He also reported that there exists a definite value of oscillation amplitude below which the lock-in does not occur even when $f_c/f_{v0}=1$. Williamson and Roshko⁽⁵⁾ examined the flow pattern in the near wake of a circular cylinder over a wide range of oscillation amplitudes by a detailed visualization experiment. They found several flow patterns in addition to the Kármán vortex at large oscillation amplitude, for instance over 50 percent of the cylinder diameter, and reported a certain hysteresis behavior of the vortex regimes. Bishop and Hassan⁽⁶⁾ and Ongoren and Rockwell⁽⁷⁾ showed that the phase difference between the circular cylinder oscillation and the lift force caused by the vortex shedding changes abruptly at a velocity within the range of synchronization. Ongoren and Rockwell⁽⁷⁾ also observed the same phase shift of vortex shedding pattern from a triangular cylinder. However, compared with circular cylinders, research on the influence of the cross-sectional configuration on the Kármán vortex excitation of a prismatic body is rather limited, as Bearman⁽⁸⁾ remarked. Earlier experiments by the present authors⁽⁹⁾ on the influence of cross-sectional configuration on the Kármán vortex excitation showed that the oscillation behaviors of a semi-circular and a triangular cylinder are greatly different from that of a circular cylinder even when other conditions such as the cylinder height, the natural frequency and the damping factor are virtually equal to each other.

The Kármán vortex excitation of an elastically supported cylinder with a small damping factor is basically a resonance which occurs when the vortex shedding frequency f_v coincides with the natural frequency of the cylinder f_n . Its mechanism can be discussed by separating it into two interactions: the interference of cylinder motion with the flow field, which affects the fluid force acting on the cylinder, and the oscillation response of the cylinder to the fluid force. These two interactions make a feedback loop which gives a self-excited oscillation feature to the cylinder motion. Among the effects of the cylinder motion on the flow, synchronization is most essential for vortex excitation since it causes f_v to coincide

with f_n at velocities at which this otherwise would not occur.

In this study, the focus is upon lock-in of the Kármán vortex caused by a small-amplitude cylinder oscillation. The transition behavior from non lock-in to lock-in is investigated by vibrating a cylinder using a mechanical oscillator which allows the cylinder oscillation amplitude to be changed. The criterion for lock-in is discussed and the threshold oscillation amplitude is determined based on this criterion.

2. Nomenclature

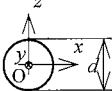
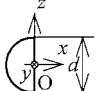
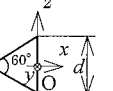
- A : Oscillation amplitude of the cylinder [mm]
- d : Characteristic length, i.e. the cylinder height, see Table 1. $d=37$ mm for water channel and $d=26$ mm for wind tunnel
- f_c : Oscillation frequency of the cylinder [Hz]
- f_v : Kármán vortex shedding frequency [Hz]
- $O-x, y, z$: Coordinate system, see Table 1
- Re : Reynolds number, $=Ud/\nu$
- R_{uu} : Cross-correlation coefficient of velocities at two locations aligned in the spanwise direction
- R_{uz} : Cross-correlation coefficient between a velocity in the near wake of the cylinder and the cylinder displacement Z
- S_u : Spectrum of velocity fluctuation in the near wake of the cylinder
- U : Free stream velocity [m/s]
- U_0 : Free stream velocity at which f_{v0} is equal to f_c [m/s]
- u : x -component of velocity in the near wake of the cylinder
- Z : Displacement of the cylinder [m]
- α : Separation angle measured from the geometrically determined most upstream point of the cylinder at rest [degree]
- ϕ_{uz} : Phase difference between u and Z
- ν : Kinematic viscosity [m²/s]
- Subscript
 - 0: Value for a fixed cylinder

3. Experimental Apparatus and Procedure

Table 1 shows cross-sectional configurations of cylinders used in this investigation. They were set in a uniform flow from left to right (in the x -direction) in a wind tunnel or a water channel. When the cylinders are fixed in a uniform flow, it is expected that the separation point movement is free on the circular cylinder surface, restricted to the upstream circular arc of the semi-circular cylinder and fixed at the downstream vertices of the triangular cylinder.

A water channel was used to find the movement of the separation point by observing the flow, which

Table 1 Cross-sectional configuration and cylinder height d of the test cylinders

	Circular cylinder	Semi-circular cylinder	Triangular cylinder
Cross sectional configuration			

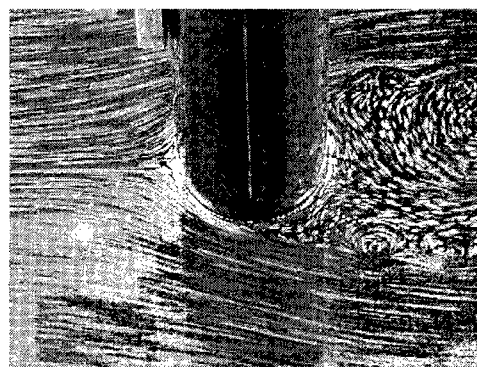
Flow direction: from left to right

was visualized by sprinkling aluminum flake on the surface. The water channel width was 400 mm and the water depth was 180 mm. The height d of cylinders used in this visualization experiment was 37 mm. The cylinder was mounted on a mechanical oscillator which gives a cross-flow oscillation with an arbitrary amplitude and frequency to the cylinder. A video camera was used to examine the relation between displacement of cylinder and the movement of separation point.

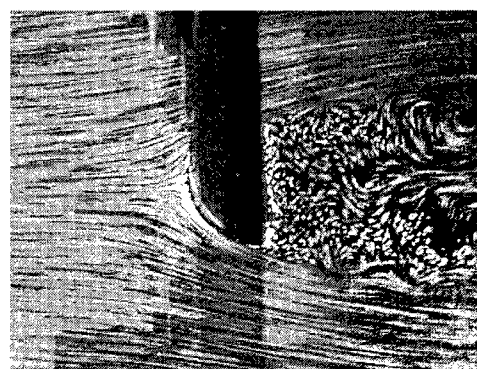
Velocity measurements were carried out in a blow-down type wind tunnel with a measuring section of 320(H) \times 320(W) \times 1 000(L) mm. The turbulence level was less than 0.6% at free stream velocity $U = 2.0$ m/s. A ring type vortex anemometer⁽¹⁰⁾ was applied to measure U . The test cylinder was installed horizontally and perpendicularly to the free stream. The height d of each cylinder was 26 mm and the blockage ratio was about 8%. The cylinder was supported at both ends outside the measuring section in one of two ways, i.e. either rigidly fixed or mounted on the mechanical oscillator for controlled oscillation experiments. End plates were attached to the cylinder to remove influence of flow through slots on the side of the measuring section⁽¹¹⁾. The motion of cylinder given by the oscillator was confined to translational oscillation in the vertical direction, i.e. a cross-flow oscillation. The mechanical oscillator allows the oscillation amplitude A and the frequency f_c to be set at respective desired values continuously and independently without stopping the experimental operation.

The cylinder displacement Z was measured by laser displacement meters at both ends. It was confirmed that rotational mode motion was not included in the cylinder oscillation since Z signals at both ends always coincided.

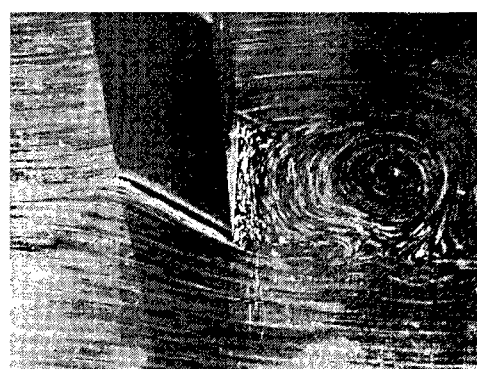
The velocity fluctuation u in the direction of the free stream was measured by constant temperature type hot-wire anemometers at locations in the near wake of the cylinder. The Kármán vortex shedding frequency f_v was obtained by applying FFT analysis to u . The spectrum S_u was obtained by averaging 20 measurements.



(a) Circular cylinder



(b) Semi-circular cylinder



(c) Triangular cylinder

Fig. 1 Visualization of separation point on the cylinders at rest ($Re = 4\,000$)

4. Results and Discussion

4.1 Visualization of the separation point

Figure 1 reproduces visualization photographs of the flow around fixed cylinders in the water channel. The flow is from the left to the right and the Reynolds number Re is about 4 000. For the circular and the semi-circular cylinders significant periodic motion of separation points was not observed when they were fixed, that is, the separation angle α measured from the geometrically-determined most upstream point was fixed at around 80 degrees regardless of vortex shedding. The separation points of the triangular

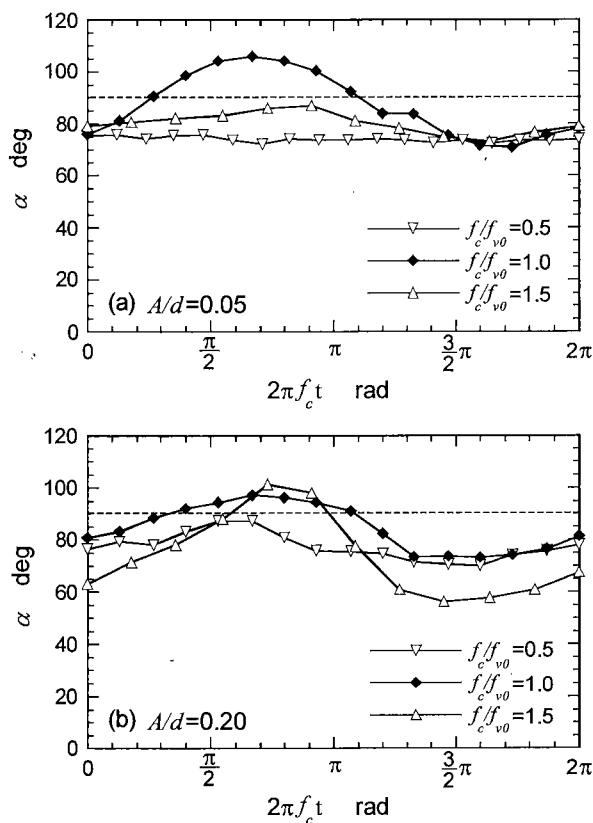


Fig. 2 Separation point movement on the oscillated circular cylinder ($Re=4000$)

cylinder were fixed on the rear vertices.

When the circular cylinder and the semi-circular cylinder oscillate, the separation points moved as shown in Figs. 2 and 3, where the separation angle α during one cycle is plotted against the phase angle of the cylinder oscillation. The separation angle α was measured in a visualization photograph and the results in these figures were obtained by averaging three oscillation cycles. In these figures, the closed symbols show results under lock-in and the open symbols for non lock-in states. The parameter f_c/f_{v0} is the ratio of cylinder oscillation frequency f_c to the natural vortex shedding frequency f_{v0} .

The plots for $f_c/f_{v0}=0.5$ and $f_c/f_{v0}=1.5$ in Fig. 2 (a) for the non-dimensional oscillation amplitude $A/d=0.05$ show that the separation point of the oscillating circular cylinder moves slightly when the vortex shedding does not synchronize with the cylinder oscillation. For $f_c/f_{v0}=1.0$, when lock-in occurs at this small oscillation amplitude, the separation point moves over a considerably wide region extending toward downstream including the maximum-height position, i.e. the separation angle reaches values greater than 90 degrees, and synchronizes with the cylinder oscillation. When the oscillation amplitude A is larger, the movement of separation point at lock-

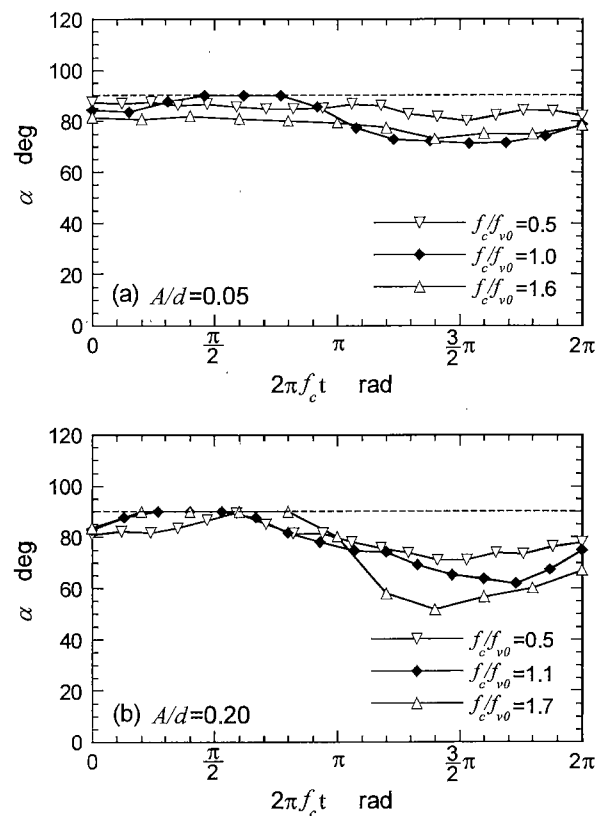


Fig. 3 Separation point movement on the oscillated semi-circular cylinder ($Re=4000$)

in is similar to that for the small A , as seen in Fig. 2 (b). It seems that the separation point movement at non lock-in becomes larger due to the influence of cylinder motion, and it becomes larger with an increase of f_c .

A similar effect of the cylinder oscillation on the separation point movement is observed for the semi-circular cylinder as shown in Fig. 3, except that the movement is confined in the region $\alpha \leq 90$ degrees, due to the geometry of the cross section. The separation point at lock-in with a small A moves more widely than at non lock-in (Fig. 3(a)). At the higher value of A as shown in Fig. 3(b), the separation point moves more widely with the increase of f_c .

In the case of the triangular cylinder, the flow always separates at the rear vertices even when the triangular cylinder is oscillated at the maximum values of A and f_c attainable in this experiment, i.e. $A/d \leq 0.2$ and $0.5 \leq f_c/f_{v0} \leq 1.5$.

4.2 Behavior of vortex shedding for variable free stream velocity

The test cylinders were oscillated in the wind tunnel at a prescribed frequency f_c and an amplitude A and the free stream velocity U was increased over a range including U_0 , at which the cylinder oscillation frequency f_c was equal to f_{v0} . Velocity fluctuation u

at a fixed position in the near wake ($x/d=2, y/d=0, z/d=1$) was detected and the vortex shedding frequency f_v was obtained from the velocity spectrum S_u . The cross correlation R_{uz} between u and the cylinder displacement Z , and the phase difference ϕ_{uz} between them, were also obtained from u and Z .

In Fig. 4, f_v , R_{uz} and ϕ_{uz} are plotted against U for the circular cylinder when the cylinder was oscillated at $f_c=15.7$ Hz and $A=2.3$ mm (dimensionless amplitude $A/d=0.087$). The vortex shedding frequency from its fixed counterpart, f_{v0} , is also plotted in Fig. 4(a).

In the f_v - U curve in Fig. 4(a), the lock-in phenomenon is clearly observed over a certain velocity range including the velocity U_0 . The absolute value of R_{uz} is a measure of how intensely fluctuations in velocity u and Z are related to each other. In the velocity range for $f_v=f_c$ shown in Fig. 4(a), the absolute value of R_{uz} is considerably higher than its values outside the range (see Fig. 4(b)), meaning that fluctuation in u signal is associated with the vortex shedding synchronizing with the cylinder oscillation. R_{uz} itself changes suddenly at a velocity within the lock-in region, accompanied by sign change. This behavior is caused by the shift of ϕ_{uz} as seen in Fig. 4(c). These sudden changes in R_{uz} and ϕ_{uz} are observed at a velocity around U_0 .

Results of f_v , R_{uz} and ϕ_{uz} plotted against U for the semi-circular and the triangular cylinder oscillating with identical frequency and amplitude are shown in Figs. 5 and 6. The features observed for the circular cylinder, i.e. the wide lock-in region with high absolute R_{uz} values and the abrupt change of R_{uz} with the sign change, are commonly observed for all three cylinders. A slight but significant difference is that the velocity region of lock-in for the triangular cylinder is broader than that for the circular and the semi-circular cylinder. The results of ϕ_{uz} for the triangular cylinder in Fig. 6 correspond to visualization of vortex formation around the oscillated triangular cylinder by Ongoren and Rockwell⁽⁴⁾. From Figs. 4 to 6, it can be confirmed that the phase shift of vortex shedding from an oscillating cylinder occurs whether the separation point moves or not, and that the movement of separation point is not an essential cause of the lock-in phenomenon. This is contrary to the common belief that lock-in is caused by the movement of the separation point.

No significant difference was observed between results for the increasing U and the decreasing U in the above measurements. Therefore, no hysteresis behavior occurs in the vortex shedding from the mechanically oscillated cylinder, although elastically-supported cylinders do exhibit hysteresis⁽¹⁰⁾. Since

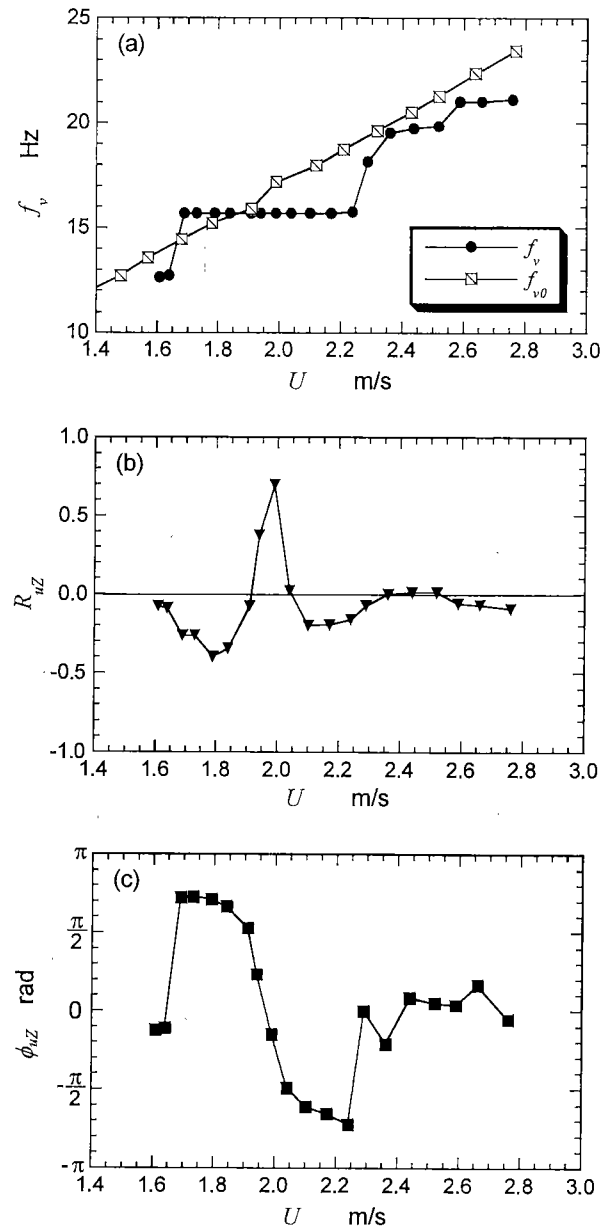


Fig. 4 f_v , R_{uz} and ϕ_{uz} against U for the circular cylinder oscillated with $f_c=15.7$ Hz and $A/d=0.087$

hysteresis is not detected here, only the results of increasing U are presented in the following figures in this paper.

4.3 Spectrum of the velocity fluctuation in the near wake of the cylinder

Figures 7 and 8 show the change of the velocity spectrum S_u for the circular cylinder when the oscillation amplitude A was increased while the flow velocity U and the oscillation frequency f_c were kept constant.

In Fig. 7, f_c is a little lower than the natural vortex shedding frequency f_{v0} (16.3 Hz). The spectrum in Fig. 7(a) is for the fixed cylinder, where a peak is seen at f_{v0} . With increasing A/d , a new sharp

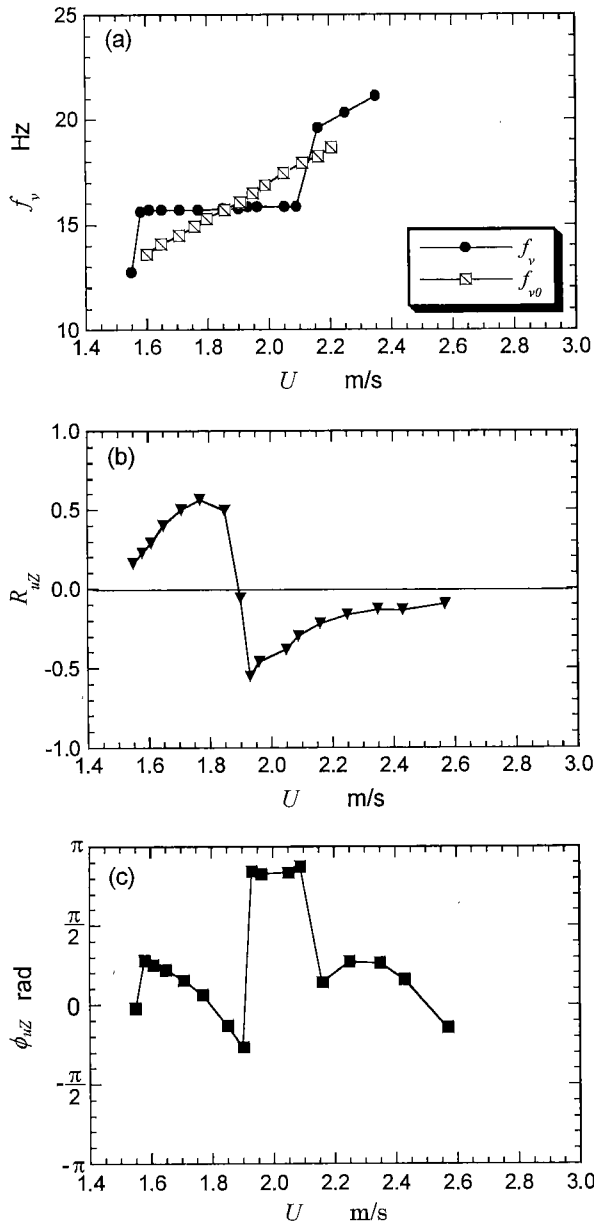


Fig. 5 f_v , R_{uz} and ϕ_{uz} against U for the semi-circular cylinder oscillated with $f_c=15.7$ Hz and $A/d=0.087$

peak at f_c begins to grow as seen in Fig. 7(b), resulting in the spectrum S_u with two peaks, a very sharp high peak at f_c and a lower and rather dull peak at around f_{v0} (Fig. 7(c)). When A/d is larger than 0.1, the two peaks merge into one sharp peak at f_c as seen in Fig. 7(d), and the peak grows higher when the amplitude is further increased. From this result, the lock-in and non lock-in states are definitely distinguished by seeing whether the spectrum has only one peak at f_c or not.

However, when f_c is set at f_{v0} , only one peak appears in a spectrum irrespective of the amplitude, as seen in Fig. 8. In this case, it seems logical that a

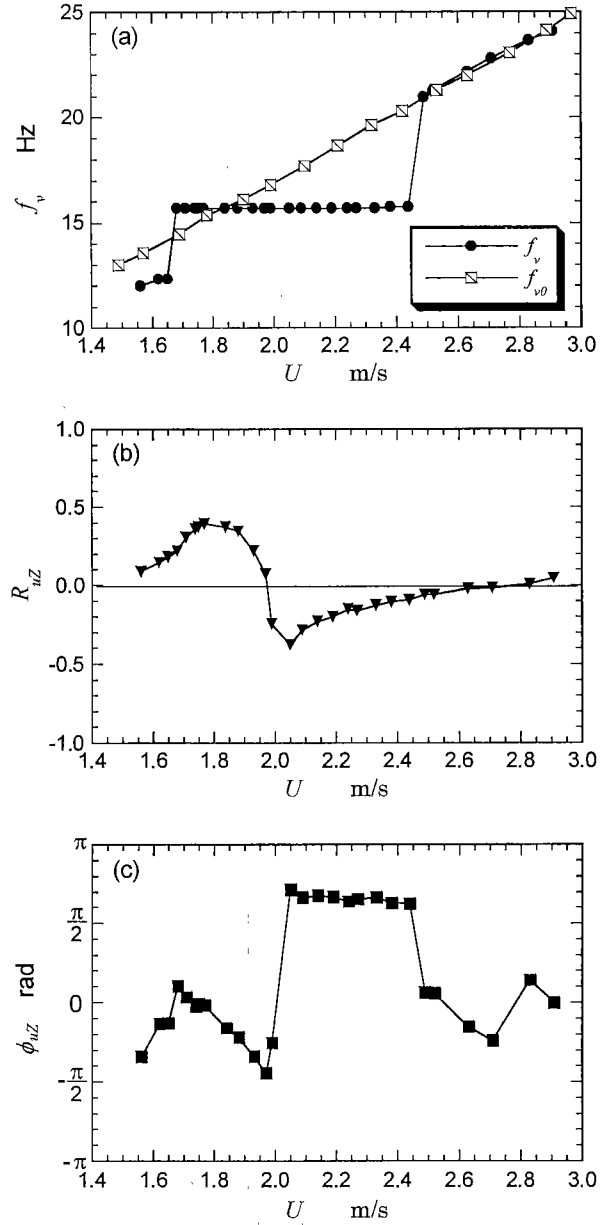


Fig. 6 f_v , R_{uz} and ϕ_{uz} against U for the triangular cylinder oscillated with $f_c=15.7$ Hz and $A/d=0.087$

single peak at f_c does not necessarily mean lock-in. The term lock-in is defined as the state of flow where vortex shedding is affected by the cylinder oscillation strongly enough to synchronize with it. Therefore, criteria other than the number of spectrum peaks are needed to determine whether lock-in occurs or not.

Since the intensity or regularity of the vortex shedding is considered to be enhanced by synchronization with the cylinder oscillation, the peak value of S_u , $(S_u)_{\text{peak}}$, may be a candidate for the criterion for lock-in. In fact, the peak of S_u at $f_c=f_{v0}$ for the oscillating cylinder is much higher than for the fixed cylinder in Fig. 8, where S_u of the fixed cylinder is shown at the

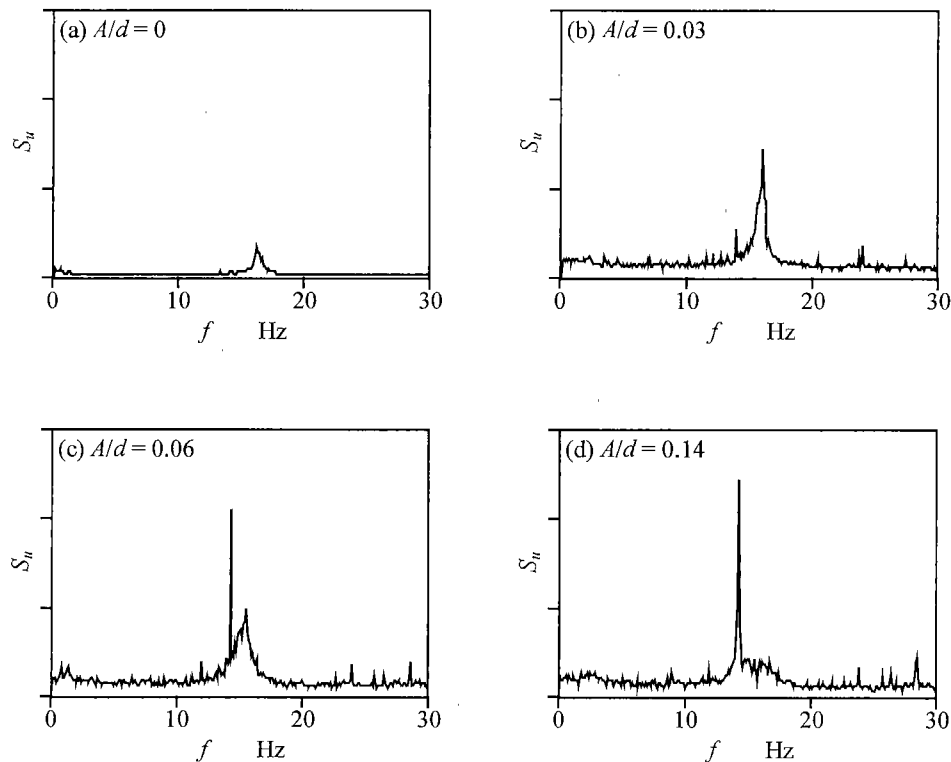


Fig. 7 Spectra of fluctuating velocity in the near wake of the circular cylinder for various oscillation amplitudes ($f_{v0}=16.3$ Hz, $f_c/f_{v0}=0.85$, $Re=3500$)

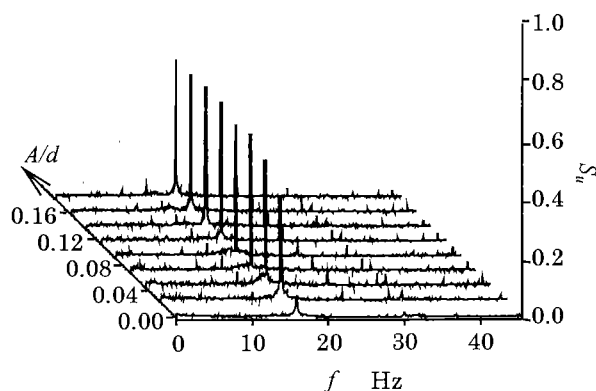


Fig. 8 Spectra of fluctuating velocity in the near wake of the circular cylinder for various oscillation amplitudes ($f_{v0}=16.3$ Hz, $f_c/f_{v0}=0.0$, $Re=3500$)

bottom.

Hence, the transitional behavior of the peak values in S_u was observed by gradually increasing the oscillation amplitude. The peak values of S_u for the oscillating cylinders are normalized by $(S_{u0})_{\text{peak}}$ at f_{v0} for their fixed counterparts. They are plotted against A/d for the three cylinders in Fig. 9. Open symbols in the figure are for the peak at f_c and closed symbols at the vortex shedding frequency f_v when S_u has both peaks. Semi-closed symbols indicate that the two peaks have merged into one at f_c .

In the case of the circular cylinder oscillating at

$f_c/f_{v0}=0.85$ and 0.90 , the peak value at f_c increases gradually with A/d while that at f_v decreases, as shown in Fig. 9(a). The latter peak vanishes when lock-in occurs. The peak value S_u at f_v for the oscillation cylinder at $A/d=0.01$, the minimum value of A/d in this experiment, is higher than $(S_{u0})_{\text{peak}}$ by a factor of four. When $f_c/f_{v0}=0.95$ and 1.00 , S_u has only one peak at f_c for the smallest value of A/d and $(S_u)_{\text{peak}}/(S_{u0})_{\text{peak}}$ increases very steeply with A/d until it attains a constant value. The value of A/d at which $(S_u)_{\text{peak}}/(S_{u0})_{\text{peak}}$ saturates gives a maximum estimation of the threshold amplitude for lock-in. The maximum threshold value thus determined from Fig. 9(a) is considerably lower than $A/d=0.05$, the minimum threshold reported by Koopman⁽⁴⁾. However, it is difficult to determine the exact amplitude threshold value at $f_c/f_{v0}=1$ since change of $(S_u)_{\text{peak}}$ is continuous.

The variation of the peak values of S_u with A/d for the other two cylinders is, roughly speaking, similar to that for the circular cylinder, as seen by comparing Fig. 9(b) and (c) with (a). A definite difference is that the increase of $(S_u)_{\text{peak}}/(S_{u0})_{\text{peak}}$ of the other two cylinders is more gradual than that for the circular cylinder, and its final value is also smaller by a factor of 2 to 4.

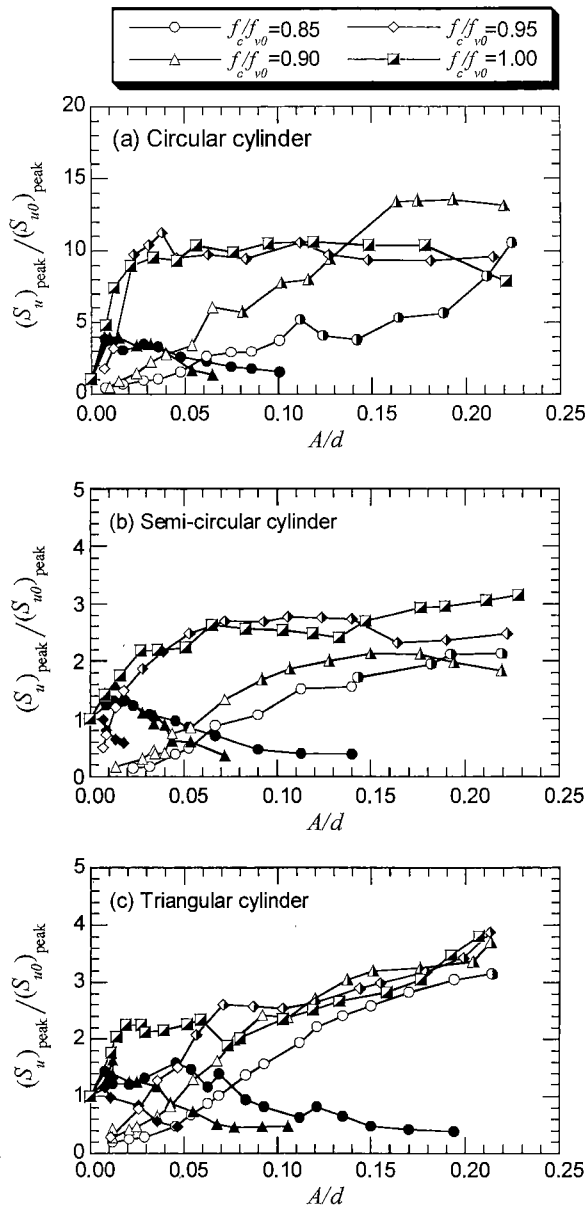


Fig. 9 The normalized spectrum peak value $(S_u)_{\text{peak}}$ of the velocity fluctuation against non-dimensional oscillation amplitude. ($Re=3500$) Open symbols and closed symbols are for $(S_u)_{\text{peak}}$ at f_c and f_v , respectively, when S_u has two peaks. Semi-closed symbols are for S_u with only one peak at $f_c=f_v$.

4.4 Spanwise cross correlation of velocity fluctuations

In order to see the effect of the cylinder oscillation on the three-dimensionality of the Kármán vortex, the velocity fluctuations were measured simultaneously at two locations with a spanwise distance of $4d$. Their cross-correlation coefficients R_{uu} are plotted against A/d in Fig. 10 for the case of $f_c/f_{v0}=1$ and a Reynolds number of about 3500. These results show that the spanwise coherency of the Kármán vortex is enhanced by the oscillation. However, a significant

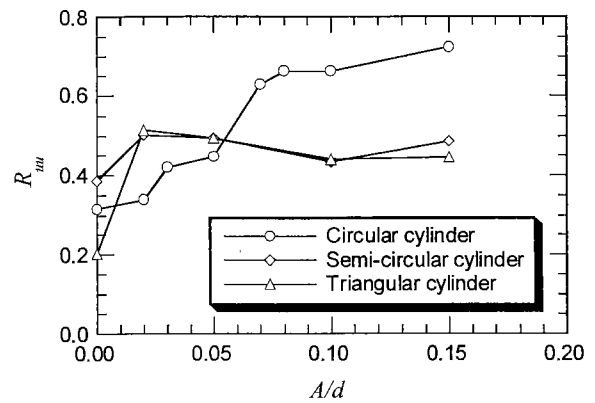


Fig. 10 The cross correlation coefficient of two velocity fluctuations measured at two locations with a spanwise distance $4d$ for $f_c/f_{v0}=1$. ($Re=3500$)

difference is seen between the circular cylinder and the other cylinders. R_{uu} for the circular cylinder increases with the increase of A/d and reaches the value of 0.6 when A/d becomes 0.07. When A/d is larger than 0.07, R_{uu} is practically constant irrespective of the oscillation amplitude. In the case of the semi-circular and the triangular cylinder, R_{uu} increases more steeply than in the circular cylinder when A/d is smaller than 0.02, and is almost constant in the range of A/d larger than 0.02.

For the circular cylinder, it is difficult to determine the amplitude threshold value for lock-in from Fig. 10 since the curve is continuous. However, it seems that the threshold is somewhere between $A/d=0.05$ and 0.07 , since the value increases abruptly in this domain. Following this reasoning, the threshold value for the semi-circular and the triangular cylinder is determined as a value lower than $A/d=0.02$.

4.5 Lock-in regions

The lock-in region on the plane of non-dimensional cylinder frequency f_c/f_{v0} and the non-dimensional amplitude A/d was investigated for all three cylinders. According to the results shown in the preceding sections, lock-in is defined by a criterion composed of the following three conditions which includes consideration of the three-dimensionality of the Kármán vortex: i) the peak of S_u at f_v is attracted to the peak at f_c , i.e. $f_c=f_v$, ii) the increase of the cross-correlation coefficient R_{uz} , and iii) the increase of the cross-correlation coefficient R_{uu} which reflects the spanwise coherency of the Kármán vortex. When all three conditions are satisfied, the Kármán vortex is judged to be locked-in with the cylinder oscillation. When none of the three conditions are satisfied, it is taken to be non lock-in. The remaining cases are defined as transition.

The results on lock-in thus obtained are shown in

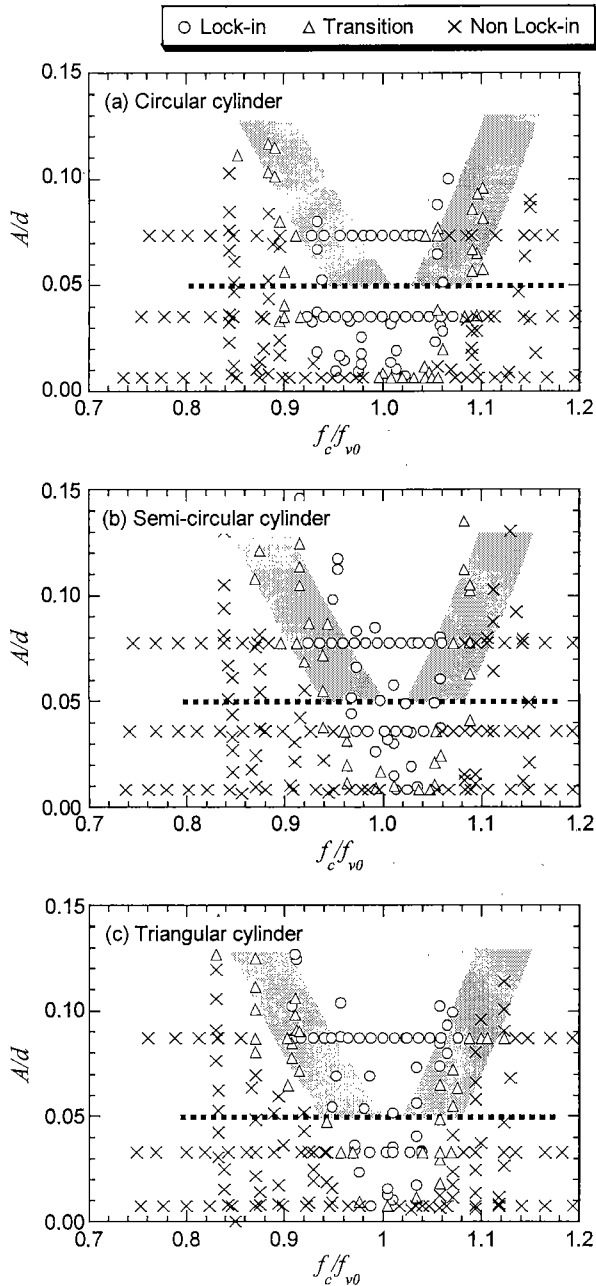


Fig. 11 The lock-in region on the plane of f_c/f_{v0} and A/d . The shading shows the lock-in region boundary and dotted line shows the minimum threshold amplitude reported by Koopman⁽⁴⁾. ($Re=3\ 500$)

Fig. 11(a), (b) and (c) for each of the cylinders. In this figure, only the data for the Reynolds number Re of about 3500, i.e. U fixed at 2 m/s, are plotted to exclude the influence of Re . The symbols which lie on a horizontal line show results obtained by increasing the oscillation frequency f_c while keeping the oscillation amplitude A constant. The symbols plotted along a vertical line show results obtained by increasing A while f_c was kept constant. In Fig. 11(a), (b) and (c), the boundary of the lock-in region, i.e. the non-

dimensional threshold amplitude given as a function of f_c/f_{v0} , for a circular cylinder reported by Koopman⁽⁴⁾ is indicated by the broad shaded line. The dotted line at $A/d=0.05$ indicates the minimum threshold amplitude reported by Koopman⁽⁴⁾. Here, Koopman's results obtained for a circular cylinder have also been plotted to Fig. 11(b) and (c) for purposes of easy comparison.

In Fig. 11(a), the lock-in region for the circular cylinder obtained in this investigation agrees well with that reported by Koopman, except for the discrepancy in the minimum threshold amplitude for the lock-in phenomenon, which here is much smaller than the value of 0.05 reported by Koopman.

As seen by comparing Fig. 11(b) and (c) with (a), the lock-in regions on the plane of f_c/f_{v0} and A/d are almost the same for all of the cylinders in spite of the large differences in the cross-sectional configuration among them. This result suggests that the large differences in the separation point movement have no effect on the lock-in phenomenon.

5. Concluding Remarks

The influence of cross-sectional configuration of a cylindrical body on the lock-in phenomenon of Kármán vortex shedding was investigated using a mechanical oscillator for cross-flow oscillation of the cylinder. A circular, a semi-circular and a triangular cylinder with an equal height were used as test cylinders to see the effect of the movement of the separation point. While the separation point can move freely for a circular cylinder, its movement is restricted to the upstream arc for a semi-circular cylinder and fixed at the rear vertices for a triangular cylinder. The following results were obtained by visualization experiments in a water channel and measurements in a wind tunnel.

(1) The separation point for the circular and the semi-circular cylinders moves very slightly irrespective of vortex shedding when they are fixed. When the vortex shedding synchronizes with the cylinder oscillation, i.e. at lock-in, the separation point for the circular cylinder moves over a considerably wide region including the maximum-height position even when the oscillation amplitude is small. In contrast, separation point movement at lock-in is restricted to the region upstream of the rear edge for the semi-circular cylinder. For the triangular cylinder, the separation point is fixed at the vertices whether the cylinder is fixed or oscillated.

(2) Lock-in phenomenon occurs within a certain free stream velocity range for all three cylinders. No hysteresis behavior is observed in the lock-in phenomenon when the velocity is increased and then de-

creased. An abrupt phase shift of vortex shedding occurs at a point within the lock-in region.

(3) A considerable increase in the cross-correlation coefficient of velocities at two locations aligned in the spanwise direction is caused by the lock-in phenomenon, which shows that the spanwise coherency of the Kármán vortex is increased by lock-in.

(4) Based on the experimental data under a fixed Reynolds number of around 3500 and the lock-in criteria including the spanwise coherency of the Kármán vortex, the lock-in regions for the three cylinders were discussed and compared with those for circular cylinders reported by Koopman⁽⁴⁾. The lock-in region on the plane of non-dimensional cylinder frequency and the non-dimensional amplitude is almost the same for all of the cylinders in spite of differences in the range of the separation point movement. The minimum value of non-dimensional threshold amplitude of the lock-in region is much smaller than the value of 0.05 which was reported so far.

Results obtained in this work imply that the movement of the separation point is a result of the lock-in phenomenon, rather than an essential cause.

References

- (1) Sarpkaya, T., Vortex Induced Oscillations, *Journal of Applied Mechanics*, 46 (1979), pp. 241-258.
- (2) Griffin, O.M. and Hall, M.S., Review-Vortex Shedding Lock-On and Flow Control in Bluff Body Wakes, *Journal of Fluids Engineering*, Vol. 113 (1991), pp. 526-537.
- (3) Funakawa, M., Excitation Mechanism of Elastically Supported Circular Cylinder in the Flow, *Bulletin of the Japan Society of Mechanical Engineering*, (in Japanese), Vol. 36, No. 285 (1970), pp. 303-312.
- (4) Koopman, G.H., The Vortex Wakes of Vibrating Cylinders at Low Reynolds Numbers, *Journal of Fluid Mechanics*, Vol. 28 (1967), pp. 501-518.
- (5) Williamson, C.H.K. and Roshko, A., Vortex Formation in the Wake of a Vibrating Cylinder, *Journal of Fluids and Structures*, 2 (1988), pp. 355-381.
- (6) Bishop, R.E.D. and Hassan, A.Y., The Lift and Drag Forces on a Circular Cylinder Oscillating in a Flowing Fluid, *Proceedings of the Royal Society of London A*, Vol. 277 (1964), pp. 51-75.
- (7) Ongoren, A. and Rockwell, D., Flow Structure from an Oscillating Cylinder Part I, Mechanisms of Phase Shift and Recovery in the Near Wake, *Journal of Fluid Mechanics*, Vol. 191 (1988), pp. 197-223.
- (8) Bearman, P.W., Vortex Shedding from Oscillating Bluff Bodies, *Annual Review of Fluid Mechanics*, Vol. 16 (1984), pp. 195-222.
- (9) Koide, M., Takahashi, T. and Shirakashi, M., Influence of Cross Sectional Configuration of a Cylindrical Body on the Kármán Vortex Excitation, *Proceedings of the 3RD ASME • JSME JOINT FLUIDS ENGINEERING CONFERENCE*, (1999), F-215, 7175.
- (10) Koide, M., Takahashi, T. and Shirakashi, M., Development of a Ring-Type Vortex Anemometer for Low-Velocity Wind Tunnel Experiments, *Bulletin of the Japan Society of Mechanical Engineering*, (in Japanese), Vol. 67, No. 657, B (2001), pp. 1105-1111.
- (11) Ishida, Y., Wakiya, S. and Shirakashi, M., Higher Velocity Resonance of Circular Cylinder in Cross Flow, *Transactions of the ASME Journal of Fluids Engineering*, Vol. 107 (1985), pp. 392-396.